Temperature dependence of photoemission from quantum-well states in Ag/V(100): Moving surface-vacuum barrier effects

M. Kralj, A. Šiber, P. Pervan, and M. Milun
Institute of Physics, P.O. Box 304, 10000 Zagreb, Croatia

T. Valla and P. D. Johnson
Physics Department, Brookhaven National Laboratory, Upton, New York 11973

D. P. Woodruff
Physics Department, University of Warwick, Coventry CV4 7AL, United Kingdom

(Received 20 October 2000; revised manuscript received 22 February 2001; published 7 August 2001)

The temperature dependence of angle-resolved photoemission from quantum-well states in ultrathin films of Ag on V(100) has been examined for films from 1–8 ML thickness within the temperature range 45–600 K. Contrary to bulk solids, the photoemission peaks shift to higher binding energy as the temperature is increased. The temperature dependence of the peak widths is linear, consistent with the expected behavior for electron-phonon coupling, but the coupling parameter λ is found to show a strong oscillatory dependence on film thickness, with some values many times larger than those found for bulk silver. The observations are explained in terms of the influence on both the initial and final states in the photoemission process of the static and dynamic movements of the surface-vacuum interface barrier induced by temperature changes.

DOI: 10.1103/PhysRevB.64.085411 PACS number(s): 79.60.Dp, 73.90.+f, 73.20.At, 79.60.Jv

I. INTRODUCTION

The ability to atomically engineer electronic potential wells through layer-by-layer growth of thin film is now allowing the exploration of some of the simplest predictions of quantum theory in a controlled fashion. Angle-resolved photoelectron spectroscopy (ARPES) has been used to characterize the binding energies of occupied quantum-well (QW) states formed by the growth of such films on metallic substrates. Momentum- (*k*-)resolved inverse photoemission spectroscopy (KRIPES) has provided complementary information on the unoccupied QW states. These experiments have done much to characterize the one-electron ground-state properties of QW states. However ARPES, as with any spectroscopy, does not truly probe the ground state, and the decay of the resulting excitation, the photohole, involves many-body effects which are also necessarily probed by the experiments. In the last few years, ARPES has been exploited to characterize these many-body coupling effects including the electron-phonon interaction which is of particular interest because of its role in conventional superconductivity.

The many-body interactions of the electronic system ultimately limit the ''lifetime'' and ''coherence length'' of the photohole excitation created in the photoemission process. This introduces a broadening and shift in energy and momentum of the corresponding spectral function

$$A(k,\omega) \propto \frac{\mathrm{Im}\,\Sigma(k,\omega)}{[\omega-\varepsilon_k-\mathrm{Re}\,\Sigma(k,\omega)]^2+[\mathrm{Im}\,\Sigma(k,\omega)]^2} \quad (1)$$

via the ''self-energy'' term $\Sigma(\mathbf{k},\omega)$. ARPES is particularly suited for studying many-body interactions in low-dimensional systems because in the case of quasi-two-dimensional systems, it directly measures the photohole spectral function given by Eq. (1). There have already been several photoemission studies quantifying many-body effects in metallic surface states and in thin films. In a study of the Mo(110) surface state[1] it was shown that all three interaction terms electron-electron, electron-phonon, and defect scattering, can be deduced from the temperature and binding energy dependence of the photoemission peak width. Other studies of metallic surface states on Cu (Refs. 2–4), Be (Refs. 5–7), Ga (Ref. 8) focused on the electron-phonon coupling term alone. The results of these studies indicate that the electron-phonon coupling constant λ (also known as the mass enhancement factor) for surface states can be significantly different from that obtained in the bulk from transport measurements. As an example, the value for the Be(0001) surface state is 3–4 times that found in bulk measurements. ARPES has also been used to study the electron-phonon coupling in QW states in films sufficiently thick (12–19 ML) for the results to be judged characteristic of the bulk metal.[9,10] In the latter case some differences in values obtained for the coupling constant have been attributed to the momentum-resolved character of an ARPES measurement as opposed to a directionally averaged transport measurement.

There have been only a few studies of many body interactions in QW states in ultrathin films where variations in the degree of QW state localization may be expected to have a significant impact on the properties. These include a study of electron-phonon coupling in thin quantum wells [1 ML and 2 ML of Na on Cu (111)][11] and a study of QW states in ultrathin films of silver on V(100) varying in thickness from 1–8 ML and covering the temperature range 30–600 K.[12] The present paper reports an extension of the latter study. This particular overlayer system was chosen because the growth properties and the binding energies of the associated QW states have already been characterized in considerable detail.[13–18] The initial objective was to investigate the temperature dependence of the spectral widths of the QW peaks in order to determine how the electron-phonon coupling in such states depends on the localization of the QW states as

TABLE I. Summary of the properties of the occupied QW states seen in Ag films on V (100) up to 8 ML thickness. The binding energy and number of nodal planes are as discussed in earlier characterization (Refs. 15 and 16). The right-hand columns show results from the present study.

Film thickness (ML)	Binding energy (eV) at 90 K	No. of nodal planes	Thermal shift eV K^{-1} ($\times 10^{-4}$)	Electron-phonon coupling λ
0 (surface state)	at Fermi level	0		1.45 ± 0.15
1	1.65 ± 0.01	0	1.5	0.21 ± 0.05
2	0.58 ± 0.01	1	1.6	1.00 ± 0.03
3	no occupied state			
4	1.43 ± 0.01	2	1.0	0.28 ± 0.12
5	0.82 ± 0.01	3	1.6	0.52 ± 0.07
6	0.36 ± 0.01	4	1.8	0.44 ± 0.07
7	1.44 ± 0.01	4		
8	1.02 ± 0.01	5	1.1	0.25 ± 0.15

the film thickness is varied. However, we observe a surprising and strong *oscillatory* variation in the coupling strength with film thickness. In addition, we also note a temperature dependence in the binding energy of the QW states, which is of opposite sign to that found in photoemission from bulk systems. In almost all previous studies of this kind, the binding energies have been found to decrease with increasing temperature. It has been suggested that the thermal expansion of the crystal leads to a lowering of the electron density and thus a reduction of the Fermi energy.[19] In the present measurements, however, we see an increase in the QW binding energy with increasing temperature. We find that changes in the binding energy can be understood in terms of the role of the thermal expansion of the outermost surface layer, and that the observed variation in electron-phonon coupling can be understood as a consequence of the coupling of the QW state photohole to the vibrations of this surface barrier.

II. EXPERIMENTAL DETAILS, RESULTS, AND PRELIMINARY ANALYSIS

The experiments reported here were carried out at the National Synchrotron Light Source (Brookhaven National Laboratory) using undulator beamline U13UB which provides photon energies in the range from 12 to 23 eV. The electron energy analyser was a Scienta SES-200, which simultaneously collects a large energy and angular window ($\sim 12°$) of the photoelectrons. This system significantly reduces the time required for data acquisition and ensures that a wide range of states in k space are recorded under identical conditions. The combined instrumental energy resolution can be set to a value in the range 6–25 meV, insignificant compared to the measured QW state widths. The angular resolution was $\sim 0.2°$. The base pressure in the experimental chamber was 4×10^{-9} Pa.

A detailed description of Ag/V(100) overlayer growth system has been given elsewhere.[13–15] These studies have shown that at room temperature silver grows pseudomorphically in an ordered layer-by-layer mode when deposited onto a V(100) substrate. This growth mode is preserved for at least ten atomic layers. Above room temperature, the Stranski-Krastanov growth mode prevails, with two pseudomorphic silver monolayers serving as a substrate for Ag clusters. Above 900 K, silver desorbs from the V(100) surface. Annealing any silver film thicker than 0.5 ML deposited on an oxygen-contaminated V(100) surface to 800 K, produces an ordered and oxygen-free substrate and film.[20] In this way it is possible to produce a well-ordered and clean V(100) surface covered with a very well-ordered silver film of up to 2 ML coverage. Thicker films (three or more monolayers) were produced by room temperature deposition of silver onto the two monolayer film. While the films of 1 and 2 ML are stable up to 800 K (Ref. 14) as implied above, thicker films are stable only up to 350 K.

The V(100) surface has an electronic structure characterized by a large *s-p* band gap extending ~ 2 eV above and below the Fermi level, along the Δ_1 high symmetry directions. In Ag films deposited on this surface, QW states can form within the range of this gap. The properties of such QW states have been characterized in earlier ARPES studies, which have also determined the energy dependence of the photoemission cross sections.[15–18] With respect to the discussion in the present paper the energies and numbers of nodal planes associated with the QW states are summarized in Table I.

Figure 1 shows a typical spectral intensity plot from a 5 ML thick Ag overlayer film recorded at a photon energy of 23.8 eV. The QW state emission is seen as a state dispersing over the angular range of $\pm 6°$. The dispersion curves of the QW states obtained in the present study, together with their effective masses are shown in Fig. 2. They differ from the values reported for the 1 and 2 ML films in an earlier study.[15] The effective masses for 1 and 2 ML QW's published in Ref. 15 were reported to be 2.2 and 3.1 m^e, respectively, both values larger than those reported in the present article. The reason for the difference is that the dispersion of almost all the QW states tends to level off approximately half-way between the center and edge of the Brillouin zone, thus increasing the effective mass on moving away from the gamma point (see Fig. 9 of Ref. 15). The use of only a small number of experimental points can therefore lead to an erroneous estimate of the effective mass, as we believe was the case in the measurements in Ref. 15. In addition, both the energy

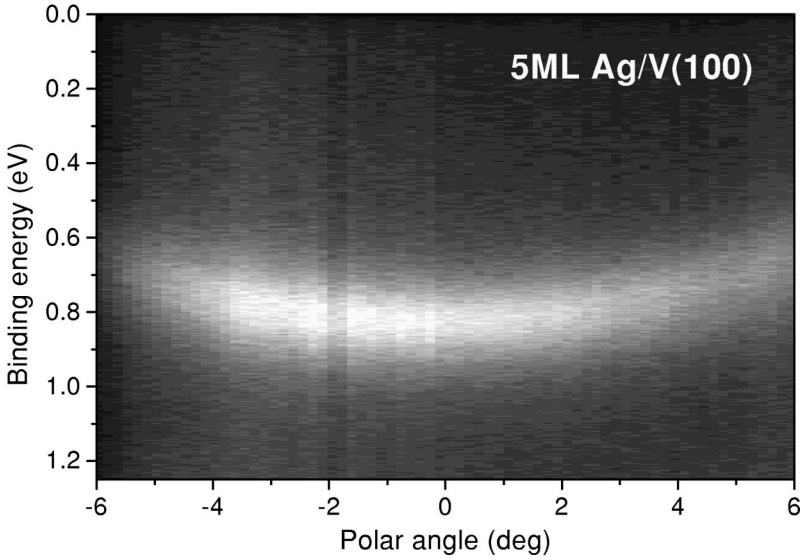

FIG. 1. Experimental photoemission intensity gray-scale maps as a function of photoelectron energy and polar emission angle collected directly from the two-dimensional detector of the Scienta concentric hemispherical electron energy analyzer from V(100) with 5 ML Ag film. The arced intensity peak corresponds to emission from the overlayer QW state at incident photon energies of 23.8 eV in a polar emission angular range of $\pm 6°$.

and angular resolution used in the present measurements are an order of magnitude better than those used in Ref. 15.

Figure 3(a) shows a typical set of normal emission spectra from a silver *s-p* derived quantum well state in a 2 ML film recorded at different temperatures. With increasing temperature the peak broadens, reduces in intensity and shifts to higher binding energies. Figure 3(b) shows plots of the energy position and peak widths as a function of temperature. Full data sets were recorded from all of the QW states listed in Table I at temperatures within the range 30–600 K. These measurements covered the full temperature range for the 1 and 2 ML films. For thicker films the maximum temperature used was 400 K because above this temperature the Stranski-Krastanov restructuring of the overlayers is fast[13] and the morphology changes to three-dimensional (3D) clusters on a 2 ML film. The temperature dependences of the peak energies are summarized in Table I.

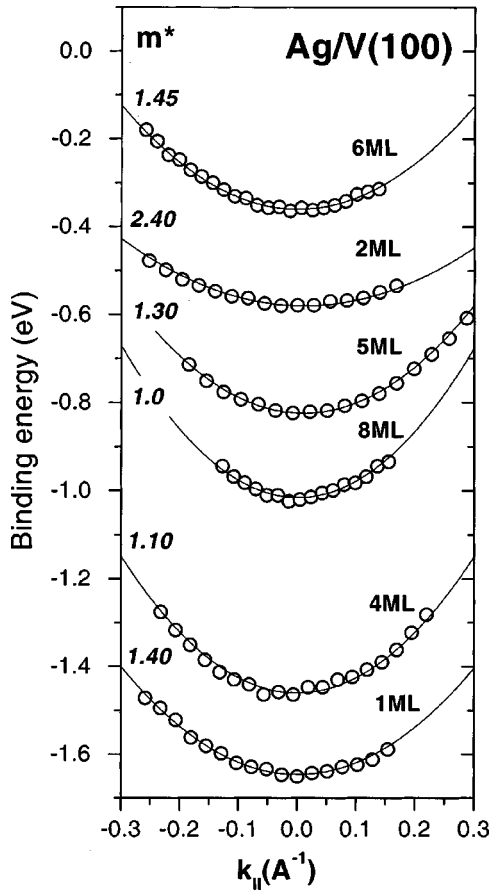

FIG. 2. Dispersion of the QW states studied in this investigation. These are extracted from the data collected by the two-dimensional detector, examples of which are shown in Fig. 1. Nearly free-electron parabola fits to the experimental points give the electron effective masses shown for each state.

We now turn to the QW peak shapes. It has been shown that the lineshape of the peaks from the QW state is completely determined by the photohole self-energy $\Sigma(\mathbf{k},\omega)$ (Ref. 21) and that the experimental spectra are accurately fitted with the ''Fermi liquid'' line shape $2\,\mathrm{Im}\,\Sigma(\omega)=\Gamma_0+2\beta\omega^2$.[21] This quasiparticle description is strictly only valid at zero temperature and at energies very close to the Fermi level,[22] but its usefulness has been found to extend to higher temperatures and a wider range of energies.[23] The energy-independent term, Γ_0, represents the sum of impurity (and/or defect) scattering and phonon scattering terms (the phonon contribution at fixed temperature gives a constant term). The quadratic term is the electron-electron contribution. By fitting to this line shape we can therefore separate out the electron-electron interaction contribution, as described more fully in Ref. 12. Briefly, we find almost the same electron-electron coupling parameter $\beta \approx 0.04\,\mathrm{eV}^{-1}$ for the QW states of 1 and 2 ML films. With these values of β, the constant term Γ_0 is found to be 150 meV for the QW state in the 1 ML film and 80–100 meV for the 2 ML film, in both cases at 60 K. Our calculations for 2 ML QW state give an electron-phonon coupling term of $\sim$40 meV for the temperature and binding energy. This leaves 40–60 meV for scattering on defects and for a contribution from the finite transmission into the substrate. We believe that in the present

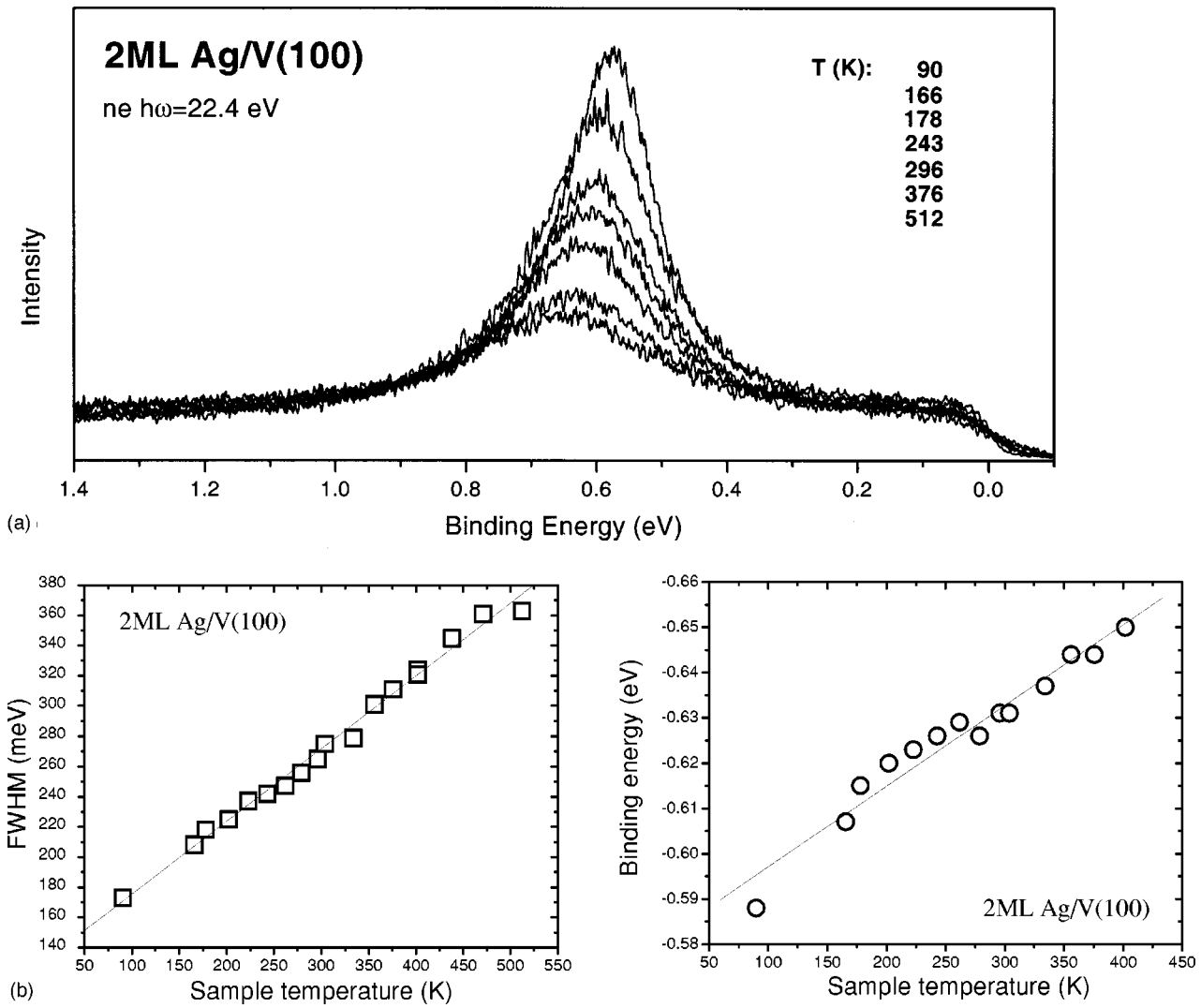

FIG. 3. (a) Normal emission photoemission spectra from the QW state corresponding to 2 ML of Ag on V(100) recorded at several different substrate temperatures. These data are extracted from a series of two-dimensional detector output maps similar to that shown in Fig. 1; (b) plots of the peak energy and peak broadening as a function of temperature deduced from a more extensive set of similar spectra.

case, the interaction of electrons with defects plays the dominant role.

The electron-phonon contribution can be deduced from the temperature dependence of the ARPES peak widths. Typical data are shown in Fig. 3, but Fig. 4 shows the result of another experiment conducted on a 5 ML Ag film deposited at 100 K without annealing. As the temperature is subsequently increased through the range 250–300 K, it is clear that some ordering of the film occurs. Note, however, that the gradient of the peak width with increasing temperature is the same before and after this restructuring. In all cases, for all film thicknesses, the temperature dependence is approximately linear at high temperatures with a gradient given by $2\pi\lambda k_B$ where λ is the electron-phonon coupling constant. Substantial differences in the coupling constant are found for the QW states in films of different thickness. These are summarized in Table I and plotted in Fig. 5 as a function of the Ag film thickness d. The most prominent feature of the $\lambda(d)$ plot is the change in the coupling strength when the thickness of the silver film is increased from 1 to 2 ML; the corresponding value of λ for the 2 ML Ag film is more than four times larger than that for the 1 ML QW state ($\lambda_{1\,\mathrm{ML}} \approx 0.23$, $\lambda_{2\,\mathrm{ML}} \approx 1.0$) and 3–4 times larger than the recently reported value measured for a 19 ML Ag film, grown on Fe(100).[9] The latter was believed to be a value characteristic of bulk Ag. Apart from the prominent maximum in λ at 2 ML, the Ag/V(100) system shows an additional maximum of the coupling constant around 5 ML.

We have also obtained new high-resolution data from the clean V(100) surface, which provide clear confirmation of the existence of the previously proposed intrinsic surface state.[24] The value of λ for this surface state 1.45 is also shown in Fig. 5. It is derived from the mass enhancement of the surface state near the Fermi level in the same manner as in the earlier surface state studies of Mo(110) (Ref. 1) and Be(0001).[5,7] This value represents one of the largest coupling constants measured in ARPES thus far and is significantly larger than the bulk value for V of 0.8.[25] However, this large electron-phonon coupling constant for the vanadium substrate cannot explain the maximum in the coupling constants

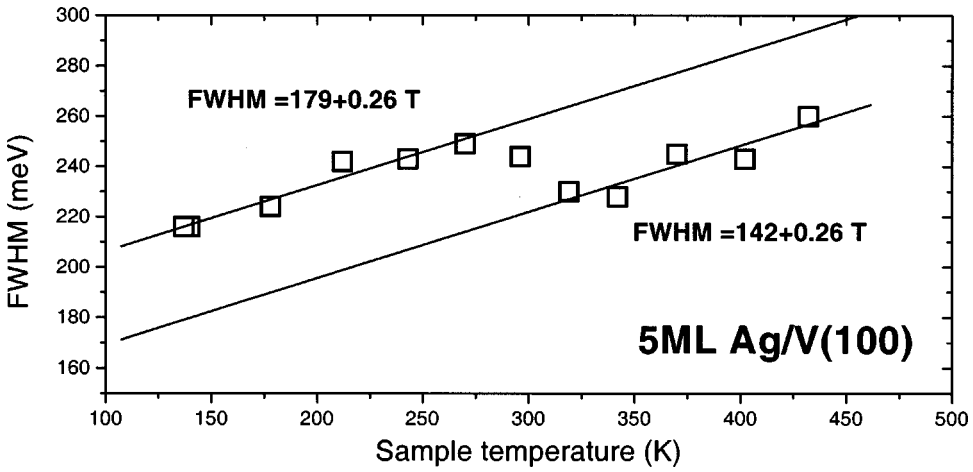

FIG. 4. Plot of the ARPES peak width as a function of substrate temperature recorded at normal emission from the QW state corresponding to 5 ML of Ag on V(100). In this experiment the original film was apparently not well ordered and the film morphology and ordering changes around 250–300 K. Note, however, that the gradient of the peak width as a function of temperature is the same before and after the restructuring.

for the thin film QW states at 2 ML. If the large $\lambda_{2\,\mathrm{ML}}$ value were solely due to the interaction of the silver overlayer with the underlying vanadium substrate, the coupling in the 1 ML film would be even stronger.

Finally note that we see a very strong oscillatory dependence of the electron-phonon coupling on the film thickness. The earlier measurements from 1 and 2 ML QW states in the Na/Cu(111) system[11] showed a small difference for the two layers, both with stronger coupling than the corresponding bulk value.

III. TEMPERATURE-DEPENDENT MOVEMENTS OF THE SURFACE-VACUUM BARRIER

A. Initial state effects

QW states of the type discussed here are simply described by the multiple reflection or ''phase accumulation'' model.[26]

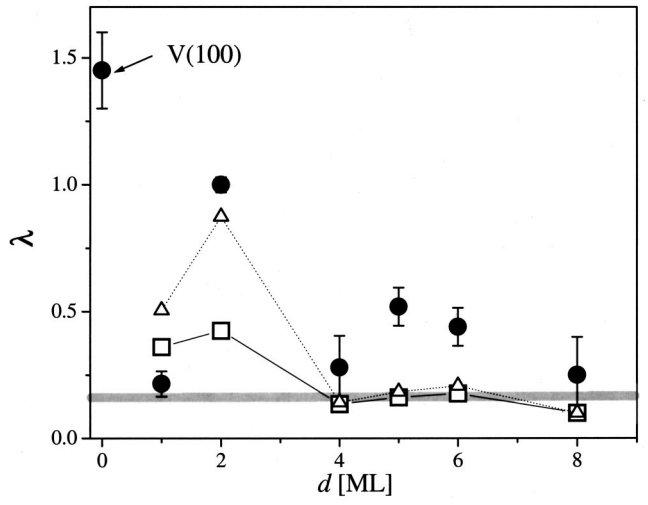

FIG. 5. The electron phonon coupling constant (λ) values obtained from Fig. 3 shown as a function of silver film thickness (solid circles). Calculated values of λ assuming an effective mass $m^*=1$ for all QWS are shown as open squares; calculated values, including experimentally determined values of the effective mass for each QW state (Fig. 2), are shown as open triangles. The experimental value of λ for the surface state on V(100) is shown at zero film thickness while λ for bulk silver is indicated by the gray line parallel to the abscissa.

The states are the bound-state solutions of Schrödinger's equation for the one-dimensional well, defined by a substrate band gap on one side and the solid vacuum interface on the other.

Within this description, it is clear that the width of the well is reflected directly in the energy of the QW bound states, there must be a matching of the electron wavelength to the well-width. The width corresponds to an integral number of half-wavelengths of the QW state wave function modified by the presence of evanescent tails extending into the substrate and the vacuum. Consider, now, the influence of thermal expansion on this system. Heating will lead to an increase in the film thickness and thus a widening of the potential well. The associated increase in the QW state wavelength results in a lower energy relative to the bottom of the well. If the Fermi energy remains fixed, the net effect is to increase the binding energy of the QW state relative to the Fermi level, as observed in the present experiments. Of course, the complete picture will reflect not only the changes in the film, but also the temperature induced changes in the substrate Fermi energy. The relative importance of these two contributions can be deduced from the thermal expansion coefficients of the two materials: $17\times10^{-6}\,\mathrm{K}^{-1}$ for Ag and $8\times10^{-6}\,\mathrm{K}^{-1}$ for V, respectively.[27] The relative difference clearly favors the dominance of the increasing Ag film thickness over the expanding substrate. The value for Ag is not strictly the one relevant to the present situation, because the Ag film is pseudomorphic centred tetragonal. The large difference in linear expansion coefficients is consistent with the fact that the cohesive energy of bulk V is almost twice as large as that of bulk Ag.[28] Indeed, if we note that for a pseudomorphic Ag film on V(100) the thermal expansion of the film parallel to the surface is constrained to the low value dictated by bulk V, we can anticipate that the expansion coefficient in the Ag film perpendicular to the surface will be even larger than that in bulk Ag.

This explanation of the binding energy shift is also consistent with the quantitative behavior for the QW states in films of different thickness. As the film thickness increases the number of nodal planes in the QW state wave function also increases (see Table I). Thus, the wavelength of the different quantum well states is very similar and the increase in wavelength induced by the thermal expansion of the film

thickness must also be approximately constant. The exception to this simple generalization is the behavior of the 1 ML Ag film. In this case it is clear that the bulk Ag thermal expansion behavior cannot be an accurate guide to the expected temperature dependence of the film thickness. Indeed, the V-Ag bonding at the interface is stronger than the Ag bulk cohesive energy (as implied by the high-temperature stability of this layer[13,14]). As such we might anticipate a lower thermal expansion of this bond than the equivalent in a bulk alloy. On the other hand, the asymmetry of the forces experienced by an atom in the outermost layer of a surface can be expected to lead to an enhanced thermal expansion coefficient (e.g., the enhanced vibrational amplitudes perpendicular to the surface[29]), as was recognized many years ago.[30]

It is rather straightforward to quantify these arguments. In the case of a simple free-electron metal the Fermi energy E_F is proportional to the reciprocal of the square of the lattice parameter. It is therefore easy to show that the temperature dependence of the Fermi energy due to thermal expansion of the crystal is given by

$$dE_F/dT = -2E_F\alpha_B, \tag{2}$$

where α_B is the coefficient of linear expansion of the solid. Applying this model to the vanadium substrate, with a value for E_F of 5.2 eV, we obtain a temperature dependence of the Fermi energy of $-8.3\times10^{-5}\,\mathrm{eV\,K^{-1}}$. The fact that vanadium is a transition metal rather than a free-electron metal, will have the effect of reducing the temperature dependence of the Fermi energy by a factor determined by the effective masses of the bands which cross the Fermi level. If the overlayer film thickness has a coefficient of thermal expansion of α_F, a QW state with an energy (relative to the bottom of the well) of E_{QW} will have a temperature dependence of

$$dE_{\mathrm{QW}}/dT = -2E_{\mathrm{QW}}\alpha_f \tag{3}$$

and taking E_{QW} as 4 eV (i.e., a binding energy relative to the Fermi level of 1.2 eV) and equating the expansion coefficient of the film thickness to the linear coefficient of bulk silver yields a result of $-13.6\times10^{-5}\,\mathrm{eV\,K^{-1}}$. This would predict an increase of the QW state binding energy relative to the Fermi level of $0.53\times10^{-4}\,\mathrm{eV\,K^{-1}}$, about a factor of 2–3 smaller than the experimentally measured values. However, the presence of the *d*-band crossing of the Fermi level in the vanadium substrate will increase this value. Further, the tetragonal distortion in the silver overlayers will result in an increase to $2.0\times10^{-4}\,\mathrm{eV\,K^{-1}}$, slightly larger than the experimental values. Note that the trends in the experimental energy shifts for the different film thickness are consistent with this model. Specifically, the shifts should be smallest for the QW states with the lowest energy relative to the bottom of the well (i.e., the largest binding energies relative to E_F), and largest for the smallest binding energy QW states. This correlation is seen in Table I, which includes both the thermal shift coefficients and the QW state binding energies.

All previous studies of the temperature dependence of bulk valence-state binding energies (e.g., Refs. 19, 31–33) have shown a decrease in binding energy with increasing temperature as noted above, and indeed the same behavior has been observed for Shockley surface states on surfaces of Cu,[2] Ag,[34] Au,[34] and Ga.[8] In contrast, an increase in binding energy with increasing temperature has been observed for *d*-like Tamm surface states on Cu(100) and $Cu_3Au(100)$.[35] However, no simple quantitative description of Tamm states, such as the phase model exists and so direct comparison is not possible. Indeed, the authors of Ref. 35 note that the shift ''most probably reflects the variation of the surface potential within the outermost layer'' and that ''quantitative estimates based on realistic three-dimensional models are not available yet.'' The observation that the occupied bulk states tend to move to lower binding energy as the temperature increases suggests that the present observation of a temperature dependent increase in the binding energy of the QW states is not due to a change in the substrate band gap. Indeed a simple application of the phase model confirms that a temperature induced reduction in the latter gap results in the QW states moving in the opposite direction to that observed.

In view of the success of the simple model in describing the temperature-dependent binding energies of the QW states, we have considered an extension to account for the observed temperature dependence of the ARPES peak widths. However, while the thermal expansion at the surface influences the well width in the same way across the whole surface, the surface phonons produce local variations in the well width which will only influence the apparent well width if the phonon wavelength is large compared with the coherence length of the QW states parallel to the surface. Such states make up only a small component of the full spectrum of surface phonons. The resulting effect on the QW state broadening is therefore negligible and we discuss this broadening only in terms of final-state electron (photohole)-phonon coupling. In the following we present a theoretical analysis that is a significantly improved approach to that given in Ref. 12. The nature of the improvement is discussed later in the text.

B. Final state effects

We find strong variation in electron-phonon coupling as a function of film thickness, and some of these coupling constants are very large relative to the value for bulk Ag [0.23 (Ref. 9)]. Within these films we expect that the largest vibrational amplitudes will be associated with the soft modes of the outermost surface layer, and as there is a large potential step at this surface-vacuum interface, it seems likely that the coupling of the photohole to this surface vibrational mode should be particularly strong.

We assume that as the surface atoms move, they locally deform the potential well seen by the electrons in the film. It is convenient to assume that the total effective potential V

can be written as a pairwise sum of the interactions between the electron and **r** and a particular crystal site j positioned at $\mathbf{r}_j$:

$$V(\mathbf{r})=\sum_j \nu(\mathbf{r}-\mathbf{r}_j). \tag{4}$$

The change of the effective potential introduced by the time dependent oscillation of the atoms in the sample can be written as

$$\Delta V(\mathbf{r})=-\sum_j \nabla\nu(\mathbf{r}-\mathbf{r}_j)\cdot\mathbf{u}_j, \tag{5}$$

where $\mathbf{u}_j$ represents the deviation of the atom at crystal site j from its equilibrium position. By expanding the atomic displacements as a superposition of normal modes characterized by the mode number s and parallel wave vector **Q**, we can evaluate the state-to-state transition amplitude per unit time w_{fi} which is defined in the first order perturbation treatment (one phonon created or destroyed in the final state of the system) by the Fermi golden rule as

$$w_{fi}=\frac{2\pi}{\hbar}|M_{fi}|^2\delta[E_f-E_i\varepsilon\hbar\omega(\mathbf{Q},s)]. \tag{6}$$

Here, M_{fi} is the matrix element of the perturbation defined by Eq. (3) calculated with the wave functions of the whole system (electrons+phonons). E_f and E_i are the final and initial energies of the electronic system. For the matrix element, M_{fi}, we can write

$$M_{fi}=\sum_j \int d^3r\Psi_f(\mathbf{r})\nabla\nu(\mathbf{r}-\mathbf{r}_j)\Psi_i(\mathbf{r}) \times\langle n_i(\mathbf{Q},s)\pm 1|\mathbf{u}_j|\mathbf{n}_i(\mathbf{Q},s)\rangle, \tag{7}$$

where Ψ_f and Ψ_i are the final and initial wave functions of the electronic system and $|n_i(\mathbf{Q},s)\rangle$ is the wave function pertaining to phonons in the crystal initial state. For the electronic wave functions we take

$$\Psi(\mathbf{r})\sim e^{i\mathbf{K}\cdot\mathbf{R}}\phi(z), \tag{8}$$

where **K** is the wave vector of the electron parallel to the surface plane and $\mathbf{r}=(\mathbf{R},z)$ where **R** is the projection of vector r onto the surface plane and z is the component perpendicular to the surface plane. $\phi(z)$ is the solution to the one-dimensional Schrödinger equation in the effective potential profile in the z direction. The single particle lifetime τ is generally given by

$$\frac{1}{\tau}=\sum_f w_{fi} \tag{9}$$

and we can calculate the effective phonon-induced width of the initial state as $\Delta E=\hbar/\tau$. The final formula for the phonon-induced lifetime of the photohole created in the QW band i is

$$\frac{1}{\tau}=\frac{A_c}{M\hbar^2}\left[\sum_f \left\{m^f_{xy}|T_{fi}|^2[2n(\omega_0)+1]\frac{Y^2(Q_{f,i})}{\omega_0}\right\} + m^i_{xy}|T_{ii}|^2[n(\omega_0)+1]\frac{Y^2(Q_{i,i})}{\omega_0}\right], \tag{10}$$

where $Q_{f,i}$ is the wave vector of the phonon emitted (or absorbed) given as

$$Q_{f,i}=\frac{\sqrt{2m^f_{xy}}}{\hbar}[E_i(\mathbf{K}=0)-E_f(\mathbf{K}=0)\pm\hbar\omega_0], \tag{11}$$

where $E_i(\mathbf{K}=0)$ and $E_f(\mathbf{K}=0)$ are the energies of the quantum well states at the bottom of the ith and fth QWS band, respectively. A_c is the area of the surface Wigner-Seitz cell, M is the mass of surface atom, and $n(\omega_0)$ is the Bose-Einstein distribution function.

Equation (10) was derived assuming that the surface atoms vibrate in the z direction with only one characteristic frequency ω_0. The effect of longitudinal surface phonons on the hole lifetime was investigated numerically and found to be much smaller than the corresponding effect from the z-polarized surface phonons. The coupling of electrons to the vibrations of the atoms located in the crystal planes below the surface plane was neglected. The dispersions of the QW states were taken to be isotropic and parabolic parallel to the surface plane with a mean effective electron mass m^f_{xy}, which depends on the particular QW state f in question. ''Recoil'' of the electron in the process of phonon emission or absorption was neglected. It was assumed that the change of the potential is uniformly distributed over the particular Wigner-Seitz cell. This assumption leads to Y factors of the form

$$Y(Q)=2A_c\frac{J_1(x_{\mathrm{ws}})}{x_{\mathrm{ws}}}, \tag{12}$$

where $x_{\mathrm{WS}}=QR_{\mathrm{WS}}$, and R_{WS} is the effective radius of the Wigner-Seitz cell. J_1 is the first-order Bessel function. If we represent the one-electron effective potential profile in the direction perpendicular to the surface with the asymmetric square well, the transition matrix element T_{fi} acquires a particularly simple form

$$|T_{fi}|^2=V_R^2|\phi_f(z=0)|^2|\phi_i(z=0)|^2. \tag{13}$$

Here, V_R is the height of the surface related (film/vacuum interface) potential step located at $z=0$.

The significance of these equations is that if an electronic state of interest is localized near the surface, and thus has a significant wave-function amplitude in the region of rapid change in potential at the surface-vacuum interface, and further if there are also final states, similarly localized, to which energy- and momentum-conserving transitions are possible, then one can expect the influence of the surface layer vibration to be strong. This argument, of course, should also be relevant to intrinsic surface states of clean surfaces and may account for the widely observed electron-phonon coupling enhancement for such states. It should be noted that Eq. (10) is equivalent to Eq. (5) from the paper by Hellsing *et al.*[36] Although the final expressions are the same, the present approach is simpler in the parametrization of the interaction matrix elements and does not rely on the results produced by the density functional calculations. It also reproduces the Q dependence of the matrix elements, accounting for the finite size of surface atoms, in a very simple and straightforward fashion, which is a consequence of the assumption of the

pairwise additivity of the electron-site potentials [Eq. (4)]. The Q dependence of matrix elements was not included in the results presented in Ref. 12 and that is the reason for differences between those results and the ones presented here. In order to evaluate Eq. (10) we have assumed that the characteristic frequency ω_0 is independent of film thickness in the range that we have explored experimentally. In the calculations we have taken $\hbar\omega_0 = 8.0\,\text{meV}$ [the Rayleigh wave phonon frequencies of Ag(111) and Ag(100) at the edge of the surface Brillouin zone are $\hbar\omega_0 \sim 8.0\,\text{meV}$ (Refs. 37 and 38)]. The asymmetric square well potential profile has a step at the film/substrate interface, which is 7.6 eV high, and another step at the film/vacuum interface (V_R) which has a height of 9.7 eV. The Fermi level is positioned at 5.6 eV above the bottom of the quantum well. We have assumed that each monolayer of Ag contributes 1.96 Å to the well width.[13–15] This potential profile reproduces both the measured binding energies of quantum well states and the magnitude of the *s-p* propagation gap into V(100).

Figure 5 shows values of the electron-phonon coupling constant derived from the slope of the calculated widths ($\hbar/\tau$) in the high temperature range. The open squares correspond to values of λ calculated assuming that the effective mass of all the QW states around the center of the Brillouin zone is equal to 1.

These theoretical results reproduce the experimentally observed oscillation of the coupling constant, even if free-electron-like dispersion of all the QW states is assumed. In this case changes in the coupling appear to arise mainly from the different localization of the states, and specifically, the amplitude of the associated wave functions at the surface barrier. These amplitudes are influenced by the QW state binding energy, the more shallow states extending further into the vacuum, and by the degree of localization as determined by the film thickness, thicker films having more extended states which (when normalized) have lower amplitudes at the surface. There is also some influence on the coupling in this simple model associated with differences in the available phase space for the photo hole decay. In particular, only a single QW state exists in the 1 ML Ag film so only intraband transitions are possible. For the thicker films both inter and intraband transitions can occur. However, calculations allowing only intraband transitions in all films produce results similar to those shown in Fig. 5, indicating that this phase space consideration is secondary.

Notice, however, that the above equations contain a dependence on the mean effective electron mass $m_{x,y}$ of each QW state, and this parameter can be extracted from our experimental determination of the dispersion of the QW state energies around normal emission. As may be seen from Fig. 2, the electron effective mass varies significantly for different states, and incorporating these values into the theoretical calculations gives the open triangles in Fig. 5. The latter are in significantly better agreement with the experimental λ. The fact that this improvement is so marked, however, is a reflection of the fact that the qualitative character of the variation of electron effective mass with thickness is actually very similar to that of λ in our experiments and in the simple theory. The origin of this $m_{x,y}$ variation is unclear. Large values of $m_{x,y}$ are typically associated with more localized states, and in the past[15,39] we have argued that the larger values seen in the thinnest films must be related to hybridization of the QW states with the substrate *d* bands. This would be favored for QW states of the highest energies close to the Fermi level, and for the thinnest films, and indeed this correlation is evident in the data of Fig. 2. Indeed, this correlation is essentially the same as that favoring an important role for the surface phonons in influencing the electron-phonon coupling. Further work, both experimental and theoretical, is clearly warranted to investigate these effects in $m_{x,y}$ more generally, but our results still clearly indicate the importance of the surface phonon coupling for the oscillatory behavior of λ values seen in our work.

IV. CONCLUSIONS

Experiments on the influence of temperature on the properties of QW states in 1–8 ML ultrathin films of Ag on V(100) show a linear dependence in both the ARPES peak energies and peak widths. The QW state binding energies, are found to increase (relative to the Fermi level) as the temperature increases, an effect opposite to that previously seen in studies of bulk bands. This can be understood as the result of two competing effects. Thermal expansion of the V substrate causes the Fermi energy to fall as the temperature rises. However, thermal expansion of the overlayer film thickness shifts the QW state energies lower. Because the expansion coefficient of the Ag film is expected to be substantially larger than that of the V substrate, the latter effect dominates and the QW state binding energies relative to the Fermi level increase with increasing temperature.

The peak width changes are explained in terms of electron-phonon coupling, but the strength of this coupling is found to show a strong and oscillatory dependence on film thickness. Simple calculations based on coupling of the photohole to the vibrational mode of the surface layer and the associated surface-vacuum potential perpendicular to the surface reproduce this behavior. The variations in electron-phonon coupling are attributable to changes in the amplitude of the QW state wave function at the surface-vacuum interface which depends on the state of localization influenced by the QW state binding energy and the spatial extent of the quantum well.

ACKNOWLEDGMENTS

The authors acknowledge the support the British Council and the Ministry of Science of Croatia (ALIS project, Grant No. Zag/984/CRO/042 to the Zagreb and Warwick groups), the Ministry of Science of Croatia (Grant No. 00350108 to the Zagreb group), the Engineering and Physical Sciences Research Council (Warwick group), and the U.S. Department of Energy Contract No. DE-AC02-98CH10886 (BNL group).

[1] T. Valla, A. V. Fedorov, P. D. Johnson, and S. L. Hulbert, Phys. Rev. Lett. **83**, 2085 (1999).
[2] B. A. McDougal, T. Balasubramanian, and E. Jensen, Phys. Rev. B **51**, 13 891 (1995).
[3] R. Matzdorf, G. Meister, and A. Goldmann, Phys. Rev. B **54**, 14 807 (1996).
[4] F. Theilmann, R. Matzdorf, and A. Goldmann, Surf. Sci. **387**, 127 (1997).
[5] S. LaShell, E. Jensen, and T. Balasubramanian, Phys. Rev. B **61**, 2371 (2000).
[6] M. Hengsberger, D. Purdie, P. Segovia, M. Garnier, and Y. Baer, Phys. Rev. Lett. **83**, 592 (1999).
[7] T. Balasubramanian, E. Jensen, X. L. Wu, and S. L. Hulbert, Phys. Rev. B **57**, R6866 (1998).
[8] P. Hofmann, Y. Q. Cai, C. Grütter, and J. H. Bilgram, Phys. Rev. Lett. **81**, 1670 (1998).
[9] J. J. Pagel, T. Miller, and T.-C. Chiang, Phys. Rev. Lett. **83**, 1415 (1999).
[10] K. Takahashi, A. Tanaka, H. Sasaki, W. Gondo, S. Suzuki, and S. Sato, Phys. Rev. B **60**, 8748 (1999).
[11] A. Carlsson, S. Å. Lindgren, C. Svensson, and L. Walldén, Phys. Rev. B **50**, 8926 (1994); A. Carlsson, B. Hellsing, S. Å. Lindgren, and L. Walldén, *ibid.* **56**, 1593 (1997).
[12] T. Valla, M. Kralj, A. Šiber, M. Milun, P. Pervan, P. D. Johnson, and D. P. Woodruff, J. Phys.: Condens. Matter **12**, L477 (2000).
[13] T. Valla and M. Milun, Surf. Sci. **315**, 81 (1994).
[14] T. Valla, P. Pervan, and M. Milun, Vacuum **46**, 223 (1995).
[15] T. Valla, P. Pervan, M. Milun, A. B. Hayden, and D. P. Woodruff, Phys. Rev. B **54**, 11 786 (1996).
[16] M. Milun, P. Pervan, B. Gumhalter, and D. P. Woodruff, Phys. Rev. B **59**, 5170 (1999).
[17] P. Pervan, M. Milun, and D. P. Woodruff, Phys. Rev. Lett. **81**, 4995 (1998).
[18] D. P. Woodruff, P. Pervan, and M. Milun, J. Phys. C **11**, L105 (1999).
[19] P. H. Citrin, G. K. Wertheim, and Y. Baer, Phys. Rev. B **15**, 4256 (1977).
[20] T. Valla, P. Pervan, and M. Milun, Appl. Surf. Sci. **89**, 375 (1995).
[21] N. V. Smith, Comments Condens. Matter Phys. **15**, 263 (1992).
[22] D. Pines and P. Nozières, *The Theory of Quantum Liquids* (Benjamin, New York, 1969).
[23] G. Grimvall, *The Electron-Phonon Interaction in Metals* (North-Holland, Amsterdam, 1981).
[24] P. Pervan, T. Valla, M. Milun, A. B. Hayden, and D. P. Woodruff, J. Phys.: Condens. Matter **8**, 4195 (1996).
[25] S. D. Brorson, A. Kazeroonian, J. S. Moodera, D. W. Face, T. K. Cheng, E. P. Ippen, M. S. Dresselhaus, and G. Dresselhaus, Phys. Rev. Lett. **64**, 2172 (1990).
[26] N. V. Smith, Phys. Rev. B **32**, 3549 (1985); Rep. Prog. Phys. **51**, 1227 (1988).
[27] *CRC Handbook of Physics and Chemistry*, 59th ed. (CRC, Boca Raton, FL, 1978).
[28] C. Kittel, *Introduction to Solid State Physics*, 5th ed. (Wiley, New York, 1976).
[29] D. P. Jackson, Surf. Sci. **43**, 431 (1974).
[30] D. P. Woodruff and M. P. Seah, Phys. Status Solidi A **1**, 429 (1970).
[31] J. A. Knapp, F. J. Himpsel, A. R. Willians, and D. E. Eastman, Phys. Rev. B **19**, 2844 (1979).
[32] N. E. Christensen, Phys. Rev. B **20**, 3205 (1979).
[33] T. Yokoya, A. Chainani, and T. Takahashi, Phys. Rev. B **55**, 5574 (1997).
[34] R. Paniago, R. Matzdorf, G. Meister, and A. Goldmann, Surf. Sci. **336**, 113 (1995).
[35] R. Paniago, R. Matzdorf, A. Goldmann, and R. Courths, J. Phys.: Condens. Matter **7**, 2095 (1995).
[36] B. Hellsing, J. Carlsson, L. Walldén, and S. A. Lindgren, Phys. Rev. B **61**, 2343 (2000).
[37] U. Harten, J. P. Toennies, and Ch. Wöll, Faraday Discuss. Chem. Soc. **80**, 137 (1985).
[38] Y. Chen, S. Y. Tong, M. Rocca, P. Morreto, U. Valbusa, K. P. Bohnen, and K. M. Ho, Surf. Sci. **250**, L389 (1991).
[39] P. D. Johnson, K. Garrison, Q. Dong, N. V. Smith, Dongqi Li, J. Mattson, J. Pearson, and S. D. Bader, Phys. Rev. B **50**, 8954 (1994).